THESIS

Menezes Sá Tarcísio Henrique

2025

Hungarian University of Agriculture and Life Sciences

Szent István Campus

Institute of Environmental Sciences

BSc Environmental Engineering

GEOSPATIAL AND HYDROLOGICAL ASSESSMENT OF SOBRADINHO RESERVOIR

Insider consultant: György Kerezsi

Assistant research fellow

Institute: Institute of Environmental Sciences

Created by: **Menezes Sá Tarcísio Henrique**

Gödöllő

2025

Table of Contents

1. Introduction and Objectives

1.1. Background

Water scarcity is one of the most pressing challenges of the twenty-first century, particularly in semi-arid regions where rainfall variability and recurrent droughts lead to severe hydrological stress. In Northeast Brazil, drought is not an occasional climatic event but a persistent feature that shapes regional development, water governance, and ecosystem resilience (Marengo et al., 2017). Within this context, the São Francisco River Basin holds national strategic importance as the largest and most economically relevant river system in the region, supplying water for agriculture, hydropower generation, domestic consumption, navigation, and fisheries. Central to this system is the Sobradinho Reservoir, which plays a vital role in regulating river flow and sustaining water availability during dry periods (Martins et al., 2011).

In recent decades, however, intensified drought conditions and increasing water demand have significantly reduced the reservoir's capacity. During the extreme drought of 2013 to 2017, one of the most severe in Brazilian history, Sobradinho lost over 60% of its surface water, equivalent to more than 2,000 km² (Martins et al., 2019). This reduction triggered cascading socio-environmental impacts, including declines in hydropower generation, water supply shortages, disruptions to irrigation, and negative effects on fisheries and local livelihoods (Vieira et al., 2018; Paredes-Trejo et al., 2021).

1.2. Relevance and Problem Statement

Drought monitoring in large reservoirs such as the Sobradinho Reservoir remains complex due to the spatial and temporal variability of hydrological responses. The reservoir is highly susceptible to drought-induced fluctuations that are uneven across its surface, creating localized hotspots of vulnerability. These variations influence water availability and surface conditions, where reduced inflow and increased sediment resuspension alter turbidity patterns and water quality (Martins et al., 2019). Such dynamics affect ecological processes, nutrient cycling, and primary productivity, leading to cascading impacts on fisheries and aquatic biodiversity (Schmitz et al., 2023).

Despite the significance of these impacts, assessing drought severity and its effects remains challenging due to the lack of standardized indices and consistent monitoring frameworks. The

diversity of drought indicators, each focusing on different hydrological aspects, often results in ambiguous interpretations and inconsistent evaluations across time and space. Therefore, harmonizing drought assessment methods is crucial to accurately capture the onset, duration, and magnitude of hydrological variability affecting the Sobradinho Reservoir, ensuring reliable information for sustainable water management and energy security (de Queiroz Santos et al., 2022; Su et al., 2017).

1.3. Research Gap

Previous studies have examined hydrological conditions, power generation, or ecological responses in isolation; however, few have conducted an integrated analysis of surface water dynamics and turbidity using geospatial and remote sensing tools over extended drought periods. Limited attention has been given to the spatial heterogeneity of drought impacts within the reservoir or to the combined use of drought indices and satellite-derived indicators to support adaptive water management.

1.4. Objectives of the Study

The overarching objective of this thesis is to evaluate and improve the understanding of drought variability and water quality dynamics in the Sobradinho Reservoir using remote sensing and geospatial analysis. Specifically, the study quantifies changes in precipitation using CHIRPS data, analyzes evapotranspiration and evaporation patterns using MODIS products, and maps spatial and temporal variations in turbidity using Landsat-8 imagery and the Normalized Difference Turbidity Index (NDTI). These indicators are integrated to assess the impacts of the 2013-2017 drought and the subsequent recovery period, providing insights into how climatic variability influences hydrological balance, water quality, and reservoir resilience in semi-arid environments.

2. Literature Review

2.1. Drought Assessment

2.1.1. Definition

Drought is a multifaceted natural phenomenon interpreted differently across scientific disciplines. It originates primarily from complex ocean-atmosphere interactions that influence regional and global climate patterns. Major drivers such as the El Niño-Southern Oscillation (ENSO), Pacific Decadal Oscillation (PDO), Atlantic Multidecadal Oscillation (AMO), Indian Ocean Dipole (IOD), and shifts in the Intertropical Convergence Zone (ITCZ) contribute to spatial and temporal variability in drought occurrences. These processes often determine the onset and persistence of meteorological droughts, which may subsequently evolve into agricultural, hydrological, or socioeconomic droughts. The severity and manifestation of these events depend not only on climatic conditions but also on the vulnerability of local ecosystems and the adaptive capacity of human societies (Abiy et al., 2019).

2.1.2. Classification

Droughts are complex natural phenomena that can be classified into several interrelated types, depending on their cause, duration, and impacts. Figure 1 illustrates the general sequence of drought occurrence and cascading effects as defined by the National Drought Mitigation Center (NDMC). All drought types originate from an initial meteorological drought, caused by a prolonged deficiency in precipitation or unfavorable climatic conditions such as high temperature, low humidity, and intense radiation. This initial phase reduces soil moisture and surface water availability, triggering agricultural drought, which affects crop productivity and vegetation health. As water deficits persist, hydrological drought develops, characterized by declining streamflow, groundwater recharge, and reservoir storage.

Figure 1. Sequence of drought occurrence and impacts (Source: NDMC)

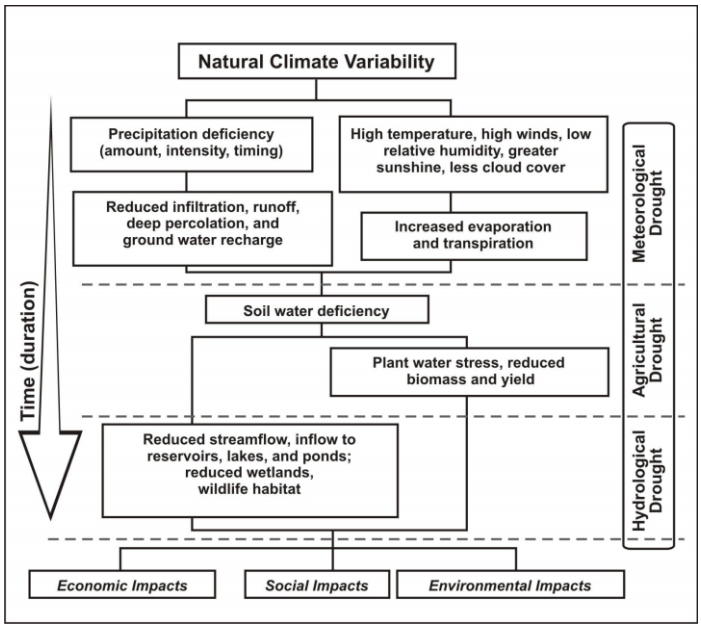

The National Drought Mitigation Center (NDMC) categorizes drought into four main types, meteorological, agricultural, hydrological, and socioeconomic drought, each representing a stage in the progression of water scarcity and its impacts (NDMC, n.d.). These forms of drought are interconnected, where meteorological anomalies often trigger subsequent agricultural and hydrological effects, ultimately leading to socioeconomic consequences.

a. Meteorological drought refers to a period of significantly below-average precipitation over a region. It is the earliest stage of drought development and is defined by the degree of dryness in comparison to a long-term average, as well as by its duration. Since precipitation varies spatially, the definition of meteorological drought is region-specific and dependent on local climatic norms.

b. Agricultural drought occurs when soil moisture becomes insufficient to meet the water needs of crops at critical stages of growth. It links meteorological conditions with agricultural impacts, resulting from a combination of reduced rainfall, increased evapotranspiration, and poor soil moisture retention. The consequences manifest as crop yield reduction, plant stress, and decreased agricultural productivity.

c. Hydrological drought develops more slowly than meteorological or agricultural drought, as it reflects the cumulative effect of prolonged precipitation deficits on surface and subsurface water resources. It is characterized by declining streamflows, reduced reservoir storage, and

lowered groundwater levels. This type of drought has long-term implications for water supply, hydroelectric generation, and ecosystem health.

d. Socioeconomic drought arises when the physical water shortage begins to affect the supply and demand of economic goods. It represents the stage where water scarcity interferes with human activities, industries, and services, such as agriculture, energy production, and domestic use, leading to economic losses and potential social conflicts. The severity of socioeconomic drought depends on societal vulnerability, management capacity, and resource dependence.

2.1.3 Drought Propagation

According to Van Loon et al. (2016), drought propagation describes how a drought evolves from one type to another as it moves through the hydrological cycle. It begins with a lack of precipitation (meteorological drought), which reduces soil moisture (agricultural drought) and eventually lowers streamflow and groundwater levels (hydrological drought). As these effects accumulate, they can lead to socioeconomic drought, where human and ecological systems experience water shortages. In simple terms, drought propagation shows that drought is not a single event but a sequence of connected processes, starting in the atmosphere and spreading across the land and water systems until it affects society and the economy.

2.1.4. Drought Indicators

Drought indicators are variables or parameters used to detect, describe, and monitor drought conditions by reflecting changes in meteorological, hydrological, and environmental systems. They include physical and biological factors such as precipitation, temperature, evapotranspiration, soil moisture, streamflow, groundwater levels, and vegetation condition (WMO & GWP, 2016).

Indicators provide the foundation for drought monitoring because they describe the current state of water availability within the hydrological cycle. For instance, precipitation and temperature records can show the onset of meteorological drought, while soil moisture, river discharge, and groundwater data reveal the progression toward agricultural and hydrological drought (NDMC, 2024).

According to the Integrated Drought Management Programme (IDMP), effective drought monitoring should use multiple indicators across various temporal and spatial scales, since drought is a complex and slow-developing phenomenon. Each indicator responds differently depending on local climate, land use, and data availability. For example, in arid regions,

evapotranspiration anomalies may signal stress earlier than precipitation anomalies (NOAA, 2020).

In summary, drought indicators serve as observational inputs that describe the physical state of the environment during dry conditions. They form the basis for drought indices, which integrate these variables into composite measures of drought severity and duration.

2.1.5. Drought Indices

Drought indices are quantitative representations of drought conditions developed from one or more indicators. They provide a standardized way to assess drought intensity, duration, and spatial extent across different regions and times. By condensing complex climate and hydrological information into a single numerical value, indices make drought monitoring and communication more consistent and accessible (WMO & GWP, 2016; NDMC, 2024).

Prominent drought indices include:

a. Standardized Precipitation Index (SPI): Measures precipitation anomalies over various time scales, making it suitable for identifying meteorological drought (McKee et al., 1993).
b. Palmer Drought Severity Index (PDSI): Uses a water balance model based on temperature and precipitation to estimate long-term drought conditions (Palmer, 1965).
c. Standardized Precipitation Evapotranspiration Index (SPEI): Extends SPI by including the effects of temperature on evapotranspiration, allowing assessment under climate warming scenarios (Vicente-Serrano et al., 2010).

Indices are integral to early warning systems and drought risk management strategies promoted by WMO, GWP, NDMC, and NOAA. They allow decision-makers to compare drought conditions globally, assess vulnerabilities, and implement proactive mitigation measures.

2.2. Monitoring Approaches

Monitoring surface water dynamics and water quality in large reservoirs requires the integration of hydrological data, records, and spatially explicit observation techniques. Traditionally, hydrological monitoring in Brazil has relied on in-situ measurements collected by the National Water and Sanitation Agency (ANA) and the National Electric System Operator (ONS), which record river discharge, reservoir levels, and operating conditions of hydropower facilities. While these observations provide accurate point-based measurements, their spatial coverage is

limited, particularly in extensive reservoirs where water levels, surface area, and turbidity can vary substantially across different sectors (ANA, 2016; ONS, 2019).

To overcome these limitations, remote sensing has emerged as a powerful monitoring approach capable of capturing hydrological and water quality changes over large spatial extents and long temporal scales. Satellite missions such as Landsat offer multispectral data at spatial resolutions suitable for mapping surface water extent, estimating turbidity, and detecting sediment concentration through spectral reflectance analyses (Pekel et al., 2016; Dogliotti et al., 2015). The Normalized Difference Water Index (NDWI) and the Modified Normalized Difference Water Index (MNDWI) have been widely used to detect surface-water bodies from multispectral imagery (McFeeters, 1996; Xu, 2006). Turbidity can be monitored using the Normalized Difference Turbidity Index (NDTI), which exploits red and green reflectance differences to detect suspended sediments (Lacaux et al., 2007).

Remote sensing applications have been increasingly adopted in Brazil to monitor water availability under drought conditions. For example, Pekel et al. (2016) produced a global surface water dataset demonstrating significant contraction of reservoir areas under prolonged droughts. In the São Francisco Basin, Martins et al. (2019) applied Landsat imagery to quantify the reduction of Sobradinho's surface area during the 2013 to 2017 drought, demonstrating the effectiveness of satellite-based monitoring in capturing hydrological responses to climatic extremes. Institutional reports by ANA (2017) and ONS (2018) underscore the importance of geospatial monitoring for water resource management, particularly during critical drought events when decisions regarding minimum flow releases must be informed by real-time information on reservoir storage and hydropower capacity.

2.3. Drought Analysis Using Remote Sensing and Climate Indices

2.3.1. The Standardized Precipitation Index (SPI)

Drought monitoring integrates meteorological observations, hydrological records, and increasingly, satellite-based indicators that capture the spatial and temporal evolution of water deficits. In semi-arid regions such as Northeast Brazil, where precipitation is irregular and surface storage is essential, understanding drought intensity and duration requires combining traditional indices with geospatial data. Classical drought classifications distinguish meteorological, agricultural, hydrological, and socio-economic droughts, depending on

whether the deficit affects precipitation, soil moisture, streamflow, or human systems (Wilhite & Glantz, 1985).

To quantify drought severity and persistence, standardized indices are widely used. The Standardized Precipitation Index (SPI) developed by McKee et al. (1993), measures precipitation anomalies by fitting long-term precipitation records to a probability distribution, commonly the gamma or Pearson Type III distribution, and then transforming them into standardized values that indicate deviations from the climatological mean. Positive SPI values denote wetter-than-normal conditions, while negative values reflect dry conditions or drought events. Because SPI relies solely on precipitation, it is straightforward to compute and requires minimal input data. This simplicity makes it particularly suitable for regions with limited meteorological records, such as the semi-arid Northeast of Brazil, where consistent temperature or soil-moisture data may be unavailable (Guttman, 1999). The SPI's standardized formulation also enables comparison of drought intensity across diverse climatic zones, providing a common reference framework for global drought assessment (Lloyd-Hughes & Saunders, 2002).

Another strength of the SPI is its ability to capture drought processes at different accumulation periods. Short-term SPI values (1-3 months) reflect meteorological or agricultural droughts that influence soil moisture and vegetation stress, while long-term scales (6-24 months) relate to hydrological and groundwater deficits that affect streamflow and reservoir storage (McKee et al., 1993). This temporal flexibility makes SPI an essential indicator for linking rainfall variability to hydrological responses such as the surface-area contraction observed in the Sobradinho Reservoir during the 2013-2017 drought.

However, several limitations arise when applying SPI to semi-arid and high-temperature environments. Because the index does not incorporate evapotranspiration or temperature effects, it may underestimate drought severity when atmospheric water demand is high, conditions typical of the São Francisco Basin. In such cases, prolonged heat and strong evaporative losses can intensify hydrological drought even when precipitation anomalies appear moderate. To address this shortcoming, complementary indices such as the Standardized Precipitation-Evapotranspiration Index (SPEI) have been proposed, which integrate temperature-driven water demand into drought characterization (Vicente-Serrano et al., 2010).

Within the context of this study, the SPI provides a robust baseline for assessing meteorological drought using CHIRPS precipitation data. It allows the identification of drought onset, duration, and intensity, which can then be related to remote-sensing indicators, such as evapotranspiration reduction (MODIS) and turbidity increases (Landsat NDTI), to evaluate how atmospheric anomalies propagate through the hydrological system of the Sobradinho Reservoir.

2.3.2. The Standardized Precipitation Evapotranspiration Index (SPEI)

The Standardized Precipitation-Evapotranspiration Index (SPEI) was developed to overcome one of the key limitations of the SPI, its omission of temperature and evapotranspiration in drought characterization. Like the SPI, the SPEI is a multi-scalar index that quantifies wet and dry conditions through statistical standardization, allowing spatio-temporal comparison of drought events across diverse climates. However, while SPI relies solely on precipitation anomalies, SPEI integrates both precipitation (P) and potential evapotranspiration (PET), effectively representing the climatic water balance ($D = P - PET$) over various accumulation periods (Vicente-Serrano et al., 2010).

By incorporating PET, the SPEI explicitly accounts for the effects of temperature on atmospheric water demand, an increasingly critical factor under global warming (Vicente-Serrano et al., 2014). PET is typically computed using the Penman-Monteith equation, which combines radiation, humidity, wind speed, and temperature to estimate potential moisture loss from the surface (Beguería et al., 2014).

The inclusion of temperature and evaporative effects makes SPEI particularly suitable for semi-arid regions such as the São Francisco Basin, where hydrological stress results not only from rainfall deficits but also from intense evaporative losses. This dual sensitivity to precipitation and temperature enables the index to capture both precipitation-driven and heat-driven droughts (Zhao et al., 2015). Furthermore, its multi-scalar design (typically 1-48 months) allows differentiation between short-term meteorological droughts and long-term hydrological or agricultural droughts, making it a powerful tool for basin-scale climate analysis.

2.3.3 Turbidity Dynamics and Remote Sensing Assessment

Turbidity is a fundamental water quality parameter that indicates the presence of suspended particulate matter (SPM), including sediments, organic detritus, phytoplankton, and dissolved substances that scatter and absorb light (Powers et al., 2023). In reservoir systems, turbidity influences primary productivity, nutrient availability, stratification processes, and aquatic

habitat conditions, making it a critical indicator for ecological integrity and water resource management (Pan et al., 2018). High turbidity levels can reduce light penetration, altering photosynthetic activity and promoting shifts in phytoplankton species composition, often favoring cyanobacteria under eutrophic and drought-stressed conditions (Nunes et al., 2022; Guedes et al., 2018). From an operational perspective, turbidity affects reservoir storage efficiency, hydropower turbine performance, and drinking water treatment costs.

In semi-arid environments such as the São Francisco River Basin, turbidity is highly responsive to hydrological fluctuations. During rainy seasons, increased river discharge introduces suspended sediments and organic matter, elevating turbidity, particularly in the upstream arms of reservoirs (Martins et al., 2019). Conversely, during droughts, receding water levels expose shallow zones to wind-driven resuspension, intensifying turbidity despite limited fluvial input (Paredes-Trejo et al., 2021).

Remote sensing has become an essential tool for turbidity assessment because suspended particles alter water reflectance in the visible and near-infrared (NIR) regions of the electromagnetic spectrum. Sentinel-2 and Landsat-8 satellites, with their multispectral capabilities, are particularly suited for monitoring inland water bodies, providing spatially continuous coverage at 10 to 30 m resolution (Pekel et al., 2016). Several spectral indices and algorithms have been developed to extract turbidity-related information from satellite reflectance data.

For quantitative turbidity retrieval, semi-analytical models such as the algorithm developed by Dogliotti et al. (2015) are widely used. This model employs a band-switching technique, using the red band for moderately turbid waters and the NIR band for extremely turbid waters, thus enabling accurate estimation across a wide turbidity gradient. The algorithm has been validated in various inland and coastal systems and has high relevance to reservoirs with strong seasonal variability, such as Sobradinho. Another widely referenced turbidity model is the generic Total Suspended Matter (TSM) algorithm proposed by Nechad et al. (2010), which, although originally calibrated on MERIS and MODIS data, has been adapted for Landsat to estimate suspended sediments in optically complex waters.

2.4. Remote Sensing and Geospatial Methods

The increasing frequency of hydrological extremes and the spatial complexity of large reservoirs have placed remote sensing at the forefront of water resource monitoring. Traditional

monitoring systems, based on hydrometric stations and sporadic field measurements, offer point-based observations that are insufficient to capture the temporal variability and spatial heterogeneity of large water bodies (ANA, 2017). In contrast, satellite-based remote sensing provides synoptic coverage across wide spatial extents and long temporal scales, making it a powerful tool for tracking reservoir surface area, drought dynamics, water quality indicators, and ecological responses (Pekel et al., 2016).

Remote sensing of inland waters is based on the interaction between electromagnetic radiation and water constituents. Pure water absorbs most wavelengths beyond the visible spectrum, while suspended sediments and chlorophyll increase reflectance, particularly in the red and near-infrared (NIR) regions (Mobley, 1999). This makes multispectral sensors such as Landsat-8 Operational Land Imager (OLI) well suited for monitoring both surface water extent and turbidity. Landsat-8 provides 30-meter resolution imagery with a 16-day revisit time, allowing for high-frequency monitoring of dynamic hydrological systems (Roy et al., 2014; Drusch et al., 2012).

Surface water extent can be delineated using spectral indices such as the Normalized Difference Water Index (NDWI) and the Modified NDWI (MNDWI), which exploit differences in reflectance between the green/NIR and green/SWIR bands to distinguish water bodies from terrestrial surfaces (McFeeters, 1996; Xu, 2006). These indices have been successfully applied in numerous studies to quantify reservoir dynamics under drought conditions, including assessments of surface water contraction in major reservoirs across Brazil (Van Den Hoek et al., 2019; Martins et al., 2019). The global surface water dataset developed by Pekel et al. (2016) using three decades of Landsat data confirms the reliability of such methods for detecting both long-term trends and abrupt hydrological changes.

For water quality monitoring, remote sensing enables spectral retrieval of turbidity, total suspended matter (TSM), and sediment load using algorithms such as the Normalized Difference Turbidity Index (NDTI) and semi-empirical models like the Dogliotti single-band switching algorithm (Dogliotti et al., 2015).

Recent advances in cloud-based geospatial computing platforms, such as Google Earth Engine (GEE), have further expanded the potential of remote sensing for hydrological analysis. GEE provides access to the full Landsat and Sentinel archives, enabling the automated processing of multi-temporal imagery and large-scale extraction of water indices. Studies demonstrate the

effectiveness of integrating GEE with Python workflows to perform time-series analysis, anomaly detection, and drought monitoring in reservoirs experiencing hydrological stress (2020; Martins et al., 2019). These tools are particularly advantageous for data-scarce regions, where remote sensing becomes the primary source of environmental information.

2.5. Study Place and Data

2.5.1. The São Francisco River Basin

As one of Brazil's most significant hydrological systems, with an estimated drainage area between 636,000 and 641,000 km², extending across the Southeast, Midwest, and Northeast regions of the country (ANA, 2016; CBHSF, 2018). The river originates in the Serra da Canastra plateau in the state of Minas Gerais, at an elevation of approximately 1,200 meters, and flows for about 2,914 kilometers before discharging into the Atlantic Ocean between the states of Alagoas and Sergipe (Britannica, 2024). Due to its latitudinal span, the basin encompasses contrasting climatic zones, with humid conditions prevailing in the upper basin and semi-arid conditions dominating the middle section. In the Northeast, annual evapotranspiration often exceeds precipitation, resulting in chronic water deficits and a high dependency on regulated surface water storage to maintain hydrological stability (ANA, 2016).

Geologically, the basin lies predominantly over the São Francisco Craton, a stable Precambrian geological formation that influences groundwater recharge, surface flow patterns, and sediment dynamics (Alkmim & Martins-Neto, 2012). The tectonic stability of this cratonic region contributed to the long-term development of the river system and its associated depositional environments. Hydrologically, the river is fed by numerous tributaries in its upper and middle reaches, although streamflow variability increases significantly as the river enters the semi-arid Northeast, where rainfall is highly seasonal and interannual variability is strongly influenced by large-scale climate oscillations (Marengo et al., 2017).

Water resource governance in the basin is coordinated through the São Francisco River Basin Water Resources Plan (2016–2025), implemented by the National Water and Sanitation Agency (ANA) and the São Francisco River Basin Committee (CBHSF). This institutional framework establishes strategic guidelines for flow regulation, drought mitigation, hydropower coordination, and water allocation for irrigation and domestic supply (ANA, 2016; CBHSF, 2018). Due to the basin's climatic vulnerability and socio-economic dependence on river flow, a series of large reservoirs have been constructed to regulate discharge.

2.5.2. The Sobradinho Reservoir

The Sobradinho Reservoir is the principal flow-regulation node of the São Francisco River in Brazil's semi-arid Northeast and one of the world's largest artificial lakes by surface area. At its nominal operating elevation (392.5 m a.s.l.), Sobradinho stores approximately 34.1 km³ of water and covers ~4,214 to 4,225 km², with a mean depth of ~8.6 m and maximum depth near 30 m (ANA, 2016; CHESF, 2022; ILEC, 2023; Correia et al., 2006). The reservoir is depicted on Figure 2. The contributing catchment area exceeds ~498,000 km² (ANA, 2016; CBHSF, 2018). Under design conditions, the system regulates downstream discharge at roughly 2,060 $m^3\ s^{-1}$, sustaining hydropower operations across the middle and lower basin (CHESF, 2022; Lima & Abreu, 2016).

Figure 2. Sobradinho visualization of the extension area (Source: https://earth.google.com)

Figure 2B. São Francisco Basin highlighting Sobradinho's position (Source: made by the author using Earth Engine, and geospatial libraries).

The associated Sobradinho Hydropower Plant, operated by CHESF, consists of six vertical Kaplan/Francis units totaling 1,050 MW, commissioned between 1979 and 1982 (CHESF, 2022; Wikipedia, 2024; ANEEL, 2021). Operational documentation reports a powerhouse length of ~250 m, a normal operating range of ~380.5-392.5 m, and usable (active) storage on the order of 28.7 km³ (CHESF, 2022; ANA, 2016). Owing to this scale, the reservoir represents over 60% of Northeast Brazil's hydropower storage capacity and plays a critical role in energy security during prolonged dry periods (Martins et al., 2019). The attributes of the reservoir are summarized in Table 1.

Table 1. Sobradinho Reservoir's Attributes Summary (Source: Adapted from CHESF, 2022; ANA, 2016; Martins et al., 2019.)

Attribute	Details
Storage Capacity	34.1 billion m³ (34.1 km³)
Surface Area	4,214 km²
Length	280 km

Width	5 to 50 km
Energy Contribution	4 billion kW/year
Environmental Impact	Changes in humidity and wind speed
Recent Challenges	Lower than average unregulated flow

Beyond energy generation, the reservoir supports one of Brazil's most productive agricultural hubs in the Petrolina and Juazeiro region, where irrigated fruit cultivation drives significant export revenue. It also sustains fisheries, provides water for urban and industrial use, and plays a key role in regional climate regulation through evaporation and surface-atmospheric interactions (Paredes-Trejo et al., 2021). However, its strategic importance also makes it highly vulnerable to hydrological stress. During the extreme drought of 2013 to 2017, water levels dropped to less than 5% of total storage capacity, resulting in reduced hydropower production, restricted irrigation supply, and increased conflicts over water allocation (Martins et al., 2019). These fluctuations in water availability are accompanied by significant changes in water quality, particularly turbidity. As reservoir levels decline, sediment concentration tends to increase due to wind-driven resuspension and reduced dilution capacity. Conversely, during high inflow periods, turbidity levels rise as a result of sediment-laden runoff. These dynamics directly affect aquatic ecosystems, hydropower operations, and water treatment costs, emphasizing the need for continuous monitoring and geospatial assessment (Schmitz et al., 2023).

2.6. Summary of Literature and Study Justification

The literature reviewed demonstrates that the Sobradinho Reservoir plays a pivotal role in the hydrological and socio-economic stability of the São Francisco River Basin, particularly under conditions of prolonged drought. Numerous studies have addressed the impacts of hydrological variability on storage capacity, hydropower generation, and ecological responses; however, several critical knowledge gaps remain unaddressed.

First, most existing studies analyze hydrological or water quality aspects in isolation, focusing either on surface water fluctuations (Martins et al., 2019; Van Den Hoek et al., 2019) or on turbidity and ecological impacts (Schmitz et al., 2023). Very few attempt an integrated assessment of both hydrological dynamics and water quality indicators over extended time periods. As a result, the combined effects of drought on reservoir surface area and turbidity remain poorly understood at the spatial scales relevant for water resource management.

Second, while drought indices such as SPI and SPEI have been applied at the basin scale to assess climate variability (Paredes-Trejo et al., 2021; Freitas et al., 2021), their direct relationship with reservoir-level changes has not been comprehensively quantified through geospatial analysis. There is a lack of studies linking climatic drought indicators with remote sensing-derived hydrological variables to identify spatial heterogeneity in drought impacts within large reservoirs.

Third, remote sensing applications on turbidity in Sobradinho remain limited, with previous efforts either focused on short-term analysis or restricted to small spatial extents (Santos et al., 2024). Although indices such as NDTI and algorithms such as Dogliotti et al. (2015) have shown high performance in other reservoirs, they have not yet been systematically applied to long-term turbidity monitoring in Sobradinho, particularly in relation to drought-driven hydrodynamic changes.

Fourth, there is insufficient temporal coverage in existing studies, many of which analyze single drought events without evaluating longer-term trends across multiple hydrological cycles. This limitation hinders the identification of patterns of resilience and vulnerability under changing climatic conditions and restricts the development of predictive models for water security.

3. Methods Used

3.1. Overview

This study integrates satellite-based remote sensing, climatic indices, and hydrological data to assess the effects of drought on the hydrological and water-quality dynamics of the Sobradinho Reservoir. All analyses were conducted using Google Earth Engine (GEE), Python (Jupyter), and QGIS, combining spatially explicit datasets covering the period 2000-2025.

Figure 3. São Francisco Basin highlighting Sobradinho Reservoir and its contour lines in the elevation of 393.5 m and 415m (Source: made by the author using QGIS).

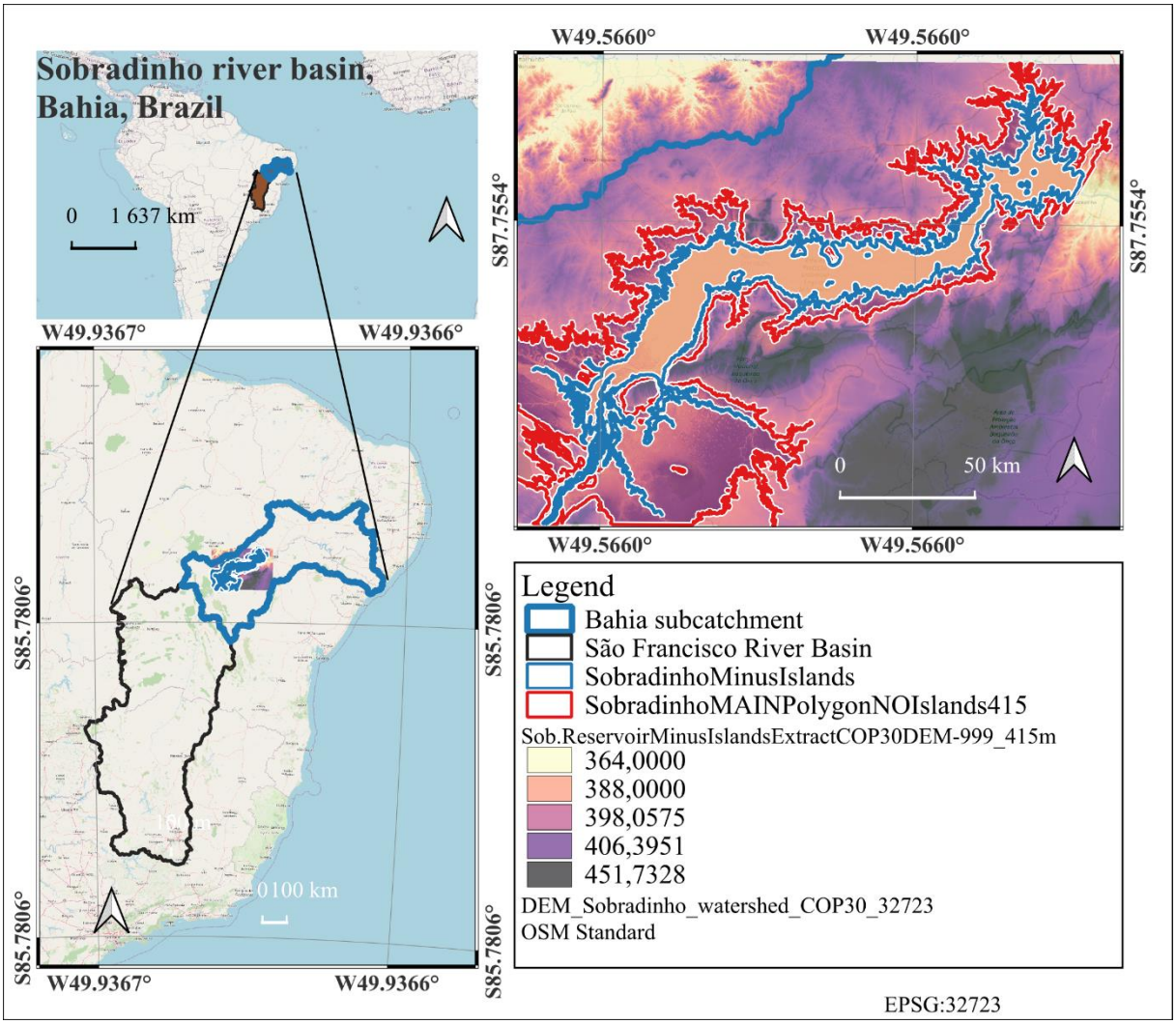

3.2. Drought Indices and Climatic Analysis

The Standardized Precipitation Index (SPI) and Standardized Precipitation–Evapotranspiration Index (SPEI) were computed to characterize drought frequency, duration, and intensity.

- SPI was calculated using CHIRPS precipitation data (0.05° resolution) aggregated to monthly scales.
- SPEI was derived from the difference between monthly precipitation (CHIRPS) and potential evapotranspiration (PET) from MOD16A2GF (500 m). PET was estimated through the Penman-Monteith approach, incorporating temperature, humidity, wind speed, and solar radiation.
- Both indices were calculated for multiple accumulation periods (3, 6, and 12 months), with SPEI-12 selected for interpretation as it best represents long-term hydrological drought (Figure 16).

Figure 16 illustrates the SPEI-12 time series for the center of the São Francisco Basin (2000–2020), highlighting the 2013-2017 extreme drought. During this period, the index remained below -1.5 for extended months, confirming severe to extreme hydrological stress that coincided with reduced inflows and record-low reservoir levels at Sobradinho.

Figure 4. SPEI-12 time series showing the 2013-2017 extreme drought in the São Francisco Basin (Source: https://github.com/tarcisiomenezes2023/THESIS_WORK Drought_Severity_map_graph)

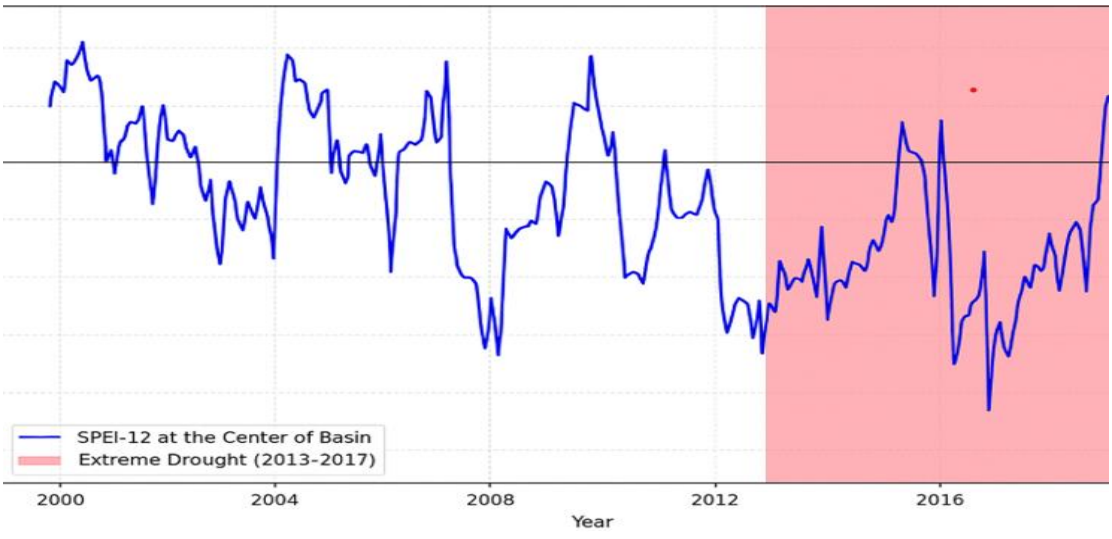

Table 2. SPEI-12 summary statistics for representative hydrological periods (2000–2024).

Period	Mean SPEI-12	Drought Classification	Notable Conditions
2000–2004	−0.43	Mild drought	Regular seasonal variability
2005–2012	−0.67	Moderate drought	Transition years with rising PET
2013–2017	−1.83	Severe to Extreme drought	Multi-year rainfall deficit, record low inflows
2018–2024	−0.28	Mild to normal	Post-drought recovery, intermittent wet peaks

This quantitative classification follows the thresholds proposed by McKee et al. (1993): values below -1 indicate moderate drought, -1.5 to -1.99 severe drought, and below -2 extreme drought. The SPI and SPEI analyses provide a robust climatic baseline for interpreting hydrological and water-quality responses in subsequent sections.

3.3. Satellite-Based Hydrological Analysis (CHIRPS, MODIS)

The hydrological analysis of the Sobradinho Reservoir catchment was based on the integration of CHIRPS precipitation data and MODIS evapotranspiration products within the Google Earth Engine (GEE) environment. These datasets were selected for their high temporal resolution, long-term availability, and validation in drought-prone semi-arid regions.

CHIRPS Precipitation Data

The Climate Hazards Group InfraRed Precipitation with Stations (CHIRPS) dataset provides quasi-global rainfall estimates at 0.05° (~5 km) resolution from 1981 to the present, merging satellite cold-cloud duration data with ground-based observations to produce bias-corrected precipitation. For this study, CHIRPS data were extracted for the Sobradinho Reservoir catchment from January 2011 to September 2025.

Daily rainfall was aggregated into monthly and annual totals, and seasonal composites were created for JFM (wet), AMJ (transition), JAS (dry), and OND (onset of rains). These operations, including temporal aggregation and zonal statistics, were conducted directly in GEE, while Python (via the GEE API and Matplotlib) was used for downloading data and generating time-series plots.

MODIS Evapotranspiration Data

Evapotranspiration dynamics were derived from the MOD16A2GF (500 m) product, which estimates actual (ET) and potential evapotranspiration (PET) using the Penman-Monteith equation. The data were aggregated to monthly and annual means for 2000-2024 and spatially clipped to the Sobradinho basin. Net evaporation was calculated as $0.8 \times PET - P$, converted to volumetric loss using the mean surface area (4,214 km²).

Elevation–Area–Capacity Curves

The methodology begins with acquiring a high-resolution digital elevation model (DEM), such as COP30, and projecting it into an equal-area coordinate system to ensure accurate surface calculations. Contour lines are generated from the DEM to identify the maximum potential inundation boundary, which is then cleaned, edited, and converted into a polygon representing the reservoir's extent. The DEM is clipped using this polygon to isolate the terrain beneath the reservoir, after which the Raster Surface Volume tool is applied in steps across elevation levels to compute the corresponding storage volume and surface area. The results from each level are compiled into a table and used to plot elevation–area–capacity curves, where storage increases with elevation, and surface area reflects the topography of the reservoir basin. This method provides a practical, DEM-based approach for water resource assessment, especially in regions lacking recent bathymetric surveys.

3.5.4. Reservoir Water Quality Analysis (Landsat – NDTI)

Water quality dynamics in the Sobradinho Reservoir were analyzed through satellite-derived turbidity using the Normalized Difference Turbidity Index (NDTI), calculated from Landsat imagery within Google Earth Engine (GEE). The NDTI exploits reflectance differences between the red and green bands to indicate suspended sediment concentrations, with higher values corresponding to higher turbidity levels.

Four representative images were selected to capture wet and dry season contrasts during the 2015-2017 drought period. Visual comparison of NDTI composites for March (wet) and September (dry) revealed substantial seasonal and interannual differences, with increased turbidity during dry months due to reduced inflows, lower storage levels, and sediment resuspension. These satellite-derived turbidity maps (Figure 18) provided valuable spatial context to the hydrological findings, linking drought-induced water level decline to the deterioration of water quality and reservoir clarity.

4. Results and Evaluation

4.1. Precipitation and Drought Patterns (2011-2025)

4.1.1. Data Overview

Precipitation data for the Sobradinho Reservoir catchment were obtained from the Climate Hazards Group InfraRed Precipitation with Station data (CHIRPS) through Google Earth Engine for the period January 2011-September 2025. The CHIRPS dataset merges satellite imagery with in-situ measurements, offering high-resolution (0.05°) daily precipitation estimates ideal for drought analysis in the semi-arid Northeast of Brazil. Daily rainfall was aggregated into monthly and annual totals and classified into four climatic trimesters: JFM (wet), AMJ (transition), JAS (dry), and OND (onset of rains).

4.1.2. Temporal Variability

The CHIRPS time series (Figure 5) reveals strong intra- and interannual rainfall variability. Precipitation is concentrated in the first quarter of the year, followed by long dry intervals with minimal rainfall. The 2013-2017 drought is marked by a sharp decline in rainfall magnitude and frequency, consistent with widespread drought conditions in the São Francisco Basin.
After 2018, precipitation frequency increases, showing gradual hydrological recovery, though isolated extremes (2016, 2020) underline the irregular convective regime typical of semi-arid climates.

Figure 5. Daily CHIRPS precipitation (2011-2025).

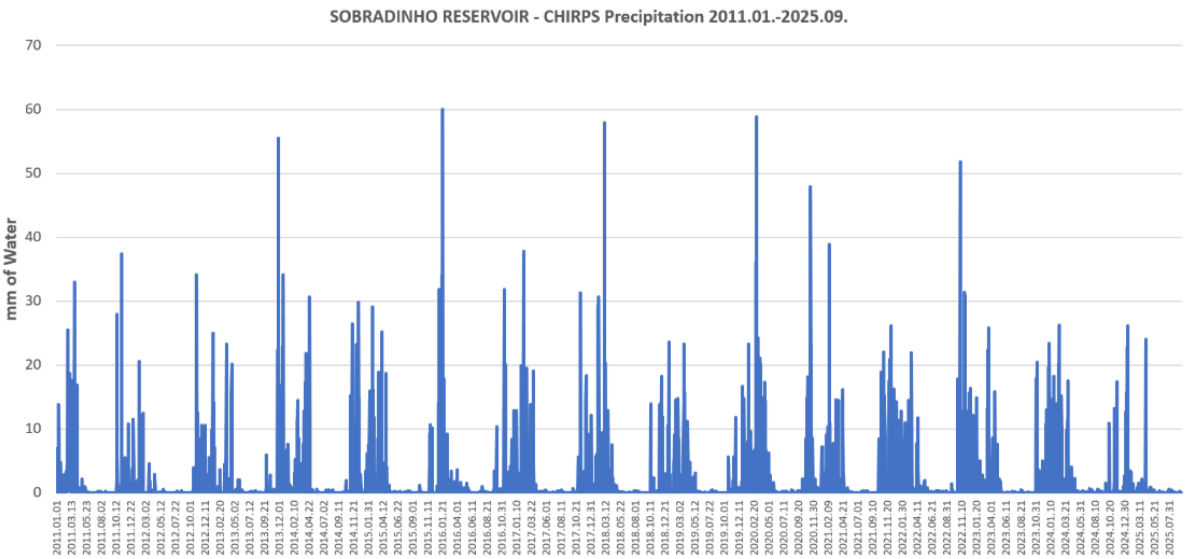

4.1.3. Monthly and Annual Precipitation Trends

Monthly data (Figure 6) show a pronounced rainfall deficit during 2013-2017, followed by a recovery phase after 2018. The annual totals (Figure 7) confirm this: minimum precipitation (< 400 mm yr^{-1}) occurs in 2012-2014 and 2016-2017, while wetter years (2019-2020) exceed 700 mm yr^{-1}. Recent years (2022-2025) show moderate rainfall (400-600 mm yr^{-1}), suggesting post-drought stabilization without full return to pre-2013 conditions.

Figure 6. Monthly cumulative CHIRPS precipitation (2011-2025).

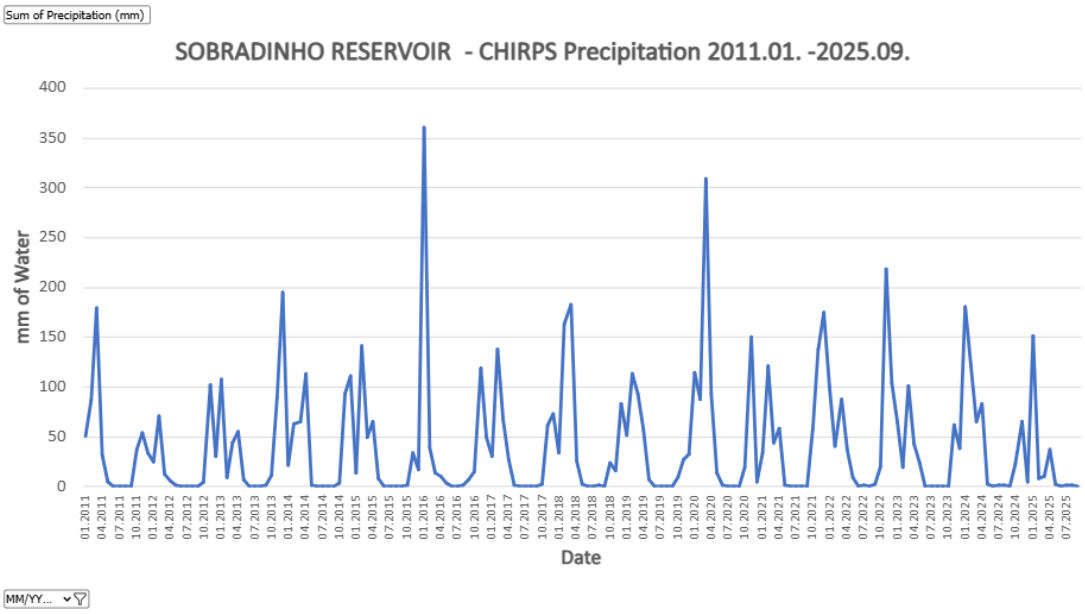

Figure 7. Annual CHIRPS precipitation totals (2011-2025).

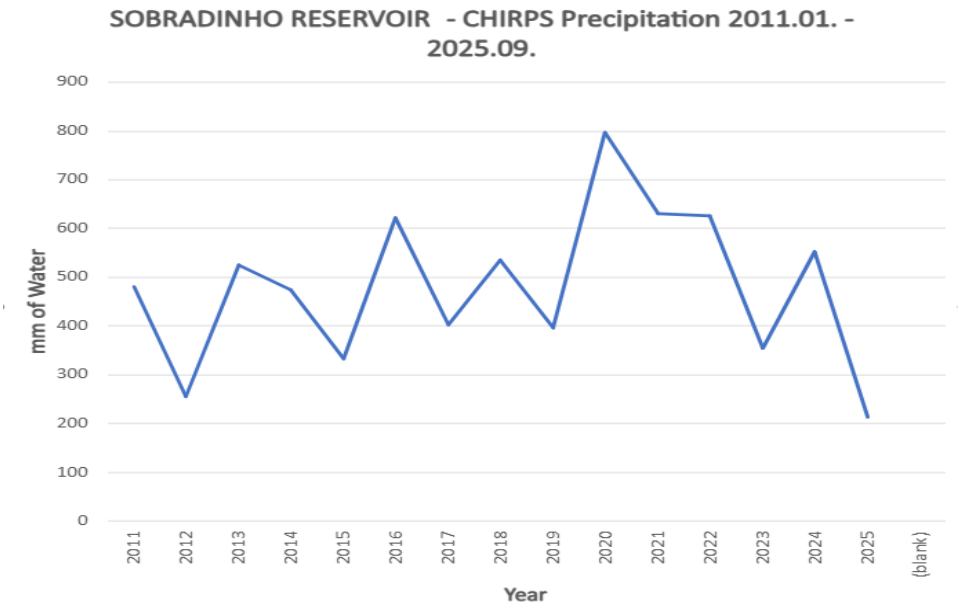

4.1.4. Seasonal Rainfall Distribution

Seasonal analysis (Figure 8) highlights JFM as the dominant rainfall period, providing most of the annual total. During 2013-2017, both JFM and OND rainfall decline sharply, indicating disruption of the normal wet-season regime. From 2018 onward, JFM recovers, though OND and AMJ remain subdued relative to pre-drought years.

Figure 8. Seasonal CHIRPS precipitation for JFM, AMJ, JAS, and OND (2011–2025).

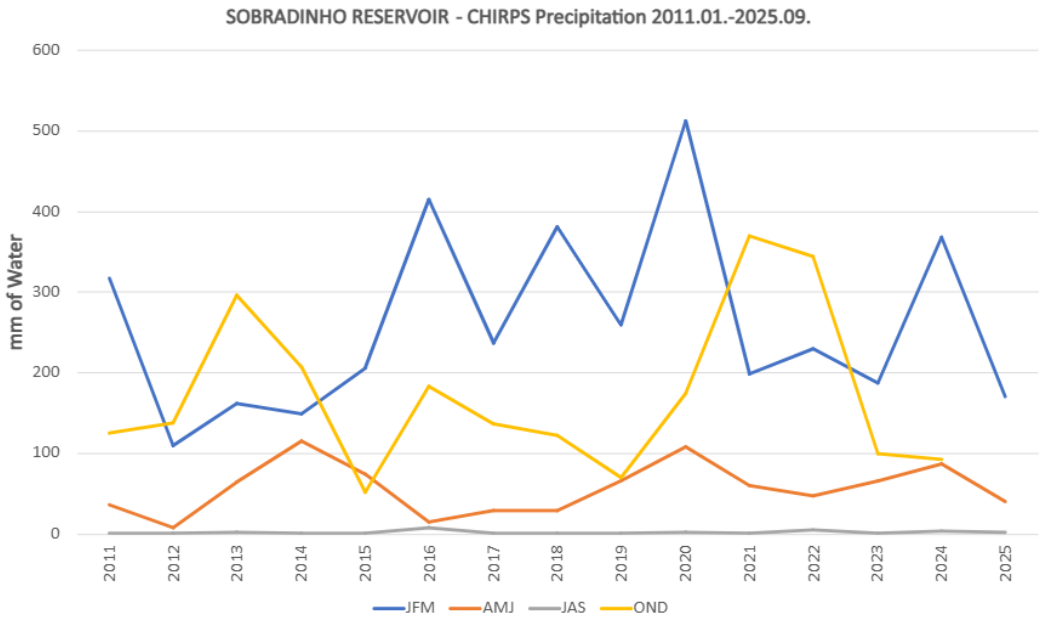

4.1.5. Average Monthly Climatology

The climatological monthly distribution (Figure 9) shows that over 70% of total annual rainfall occurs between January and March, with a secondary maximum in November-December. From May to September, rainfall is consistently below 10 mm month^{-1}, indicating a pronounced dry season lasting nearly half the year. This strong seasonal pattern directly influences reservoir inflows, evaporation rates, and hydrological storage fluctuations, which are examined in later sections.

Figure 9. Seasonal precipitation by trimester (2011-2025).

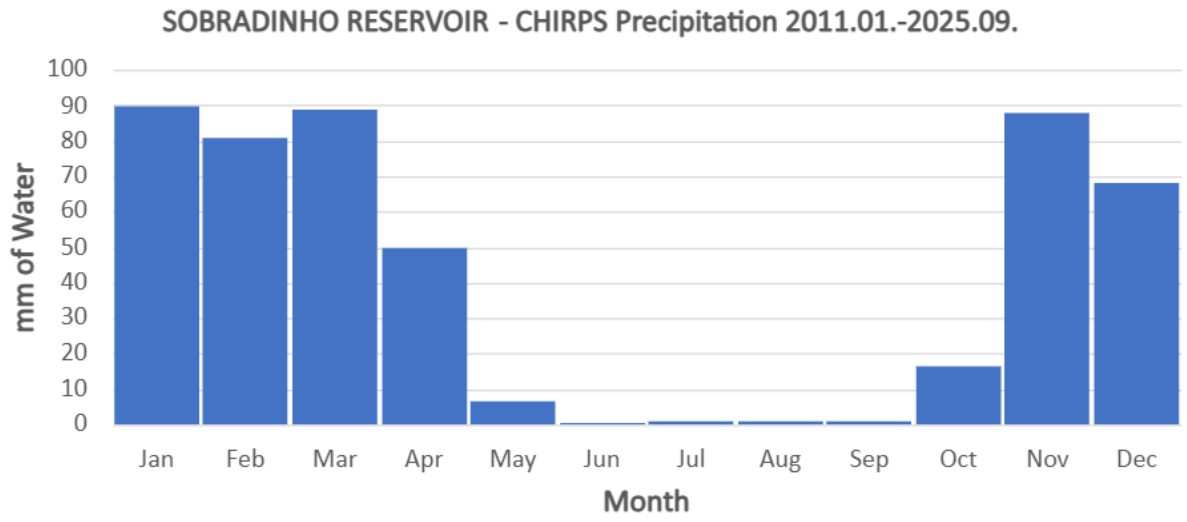

4.1.6. Interpretation and Implications

The CHIRPS precipitation analyses confirm the 2013-2017 drought as an extended multi-year anomaly characterized by persistent rainfall deficits and a breakdown of normal seasonal patterns. The post-drought phase (2018-2025) marks a transition toward recovery, with increased rainfall totals and more regular wet-season peaks. However, interannual variability remains high, suggesting that while hydrological conditions have improved, the system continues to experience significant climatic stress.

4.2. Evapotranspiration Dynamics (2000-2024)

4.2.1. Data Overview

Evapotranspiration (ET) and Potential Evapotranspiration (PET) data were derived from MODIS MOD16A2GF (500 m) via Google Earth Engine for 2000-2024. The product estimates latent heat flux using the Penman–Monteith method, integrating temperature, radiation, humidity, and vegetation indices. ET reflects actual water flux from soil and vegetation; PET represents the atmosphere's evaporative demand.

4.2.2. Temporal Evolution

Evapotranspiration (ET) and Potential Evapotranspiration (PET) data were derived from MODIS MOD16A2GF (500 m) via Google Earth Engine for 2000-2024. The product estimates

latent heat flux using the Penman-Monteith method, integrating temperature, radiation, humidity, and vegetation indices. ET reflects actual water flux from soil and vegetation; PET represents the atmosphere's evaporative demand.

Figure 10. Annual ET and PET over Sobradinho Reservoir (2000-2024, MOD16A2GF 500 m).

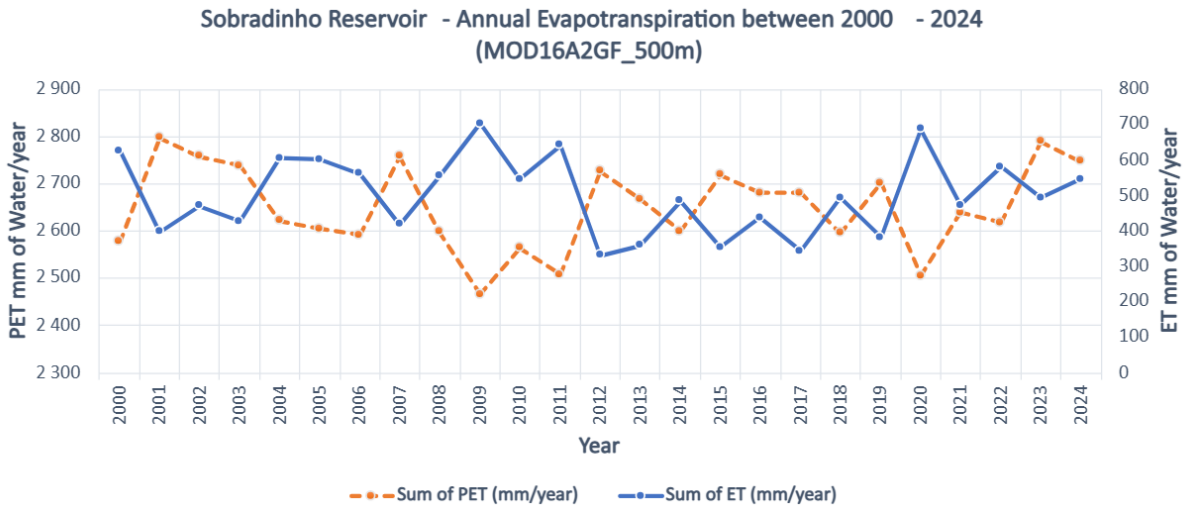

4.2.3. Monthly and Seasonal Variability

Monthly averages (Figure 6) reveal a pronounced seasonal rhythm in evapotranspiration. ET reaches its maximum during the wet season (January-March), when rainfall replenishes soil moisture and vegetation activity intensifies, supporting evapotranspiration rates close to 70-80 mm month^{-1}. In contrast, ET drops to near-zero values during the core dry season (July-September), reflecting the depletion of available water and physiological dormancy of vegetation.

PET, on the other hand, remains consistently high throughout the year, typically exceeding 200 mm month^{-1}, with a subtle increase between August and October driven by elevated solar radiation, higher air temperatures, and low atmospheric humidity. This persistent atmospheric demand underlines the strong energy-limited nature of the Sobradinho Basin: even when water availability declines, the climatic conditions continue to favor intense evaporation potential.

The mean climatology (Figure 11) further emphasizes this imbalance, showing PET peaking near 270 mm month^{-1} in October, at the end of the dry season, while ET rarely exceeds 80 mm month^{-1}, even during the rainiest months. This clear gap between potential and actual evapotranspiration quantifies the moisture deficit characteristic of semi-arid hydrological

regimes and highlights the sensitivity of the catchment's water balance to seasonal rainfall distribution.

Figures 11. Monthly and mean climatology of ET and PET (2000–2024).

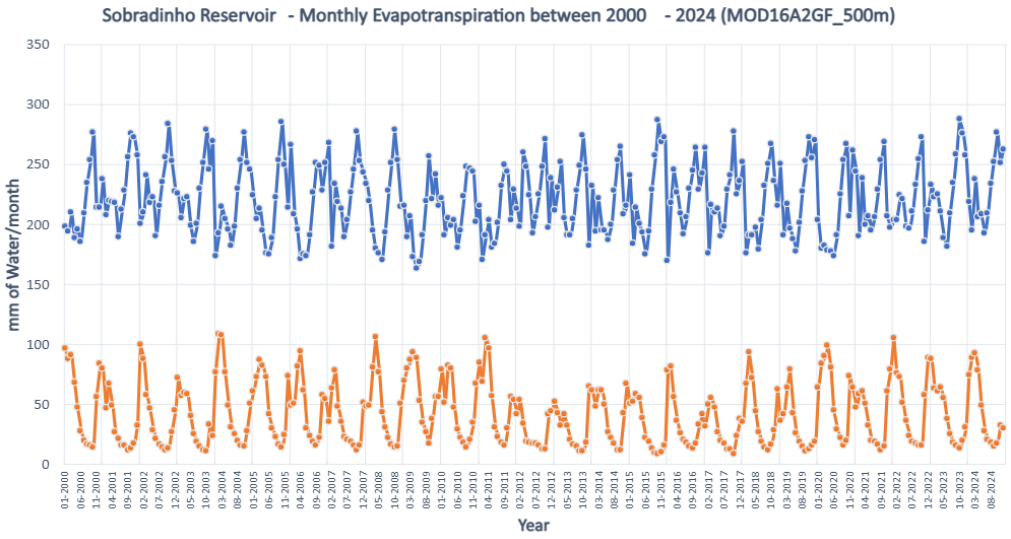

The mean monthly climatology (Figure 12) confirms that atmospheric water demand (PET) consistently exceeds available moisture (ET) throughout the year. PET reaches its maximum (≈ 270 mm month^{-1}) in October, coinciding with the end of the dry season. ET remains below 80 mm month^{-1} even during wet months, highlighting strong evaporative stress typical of semi-arid hydrological regimes.

Figure 12. Mean monthly ET and PET climatology (2000-2024).

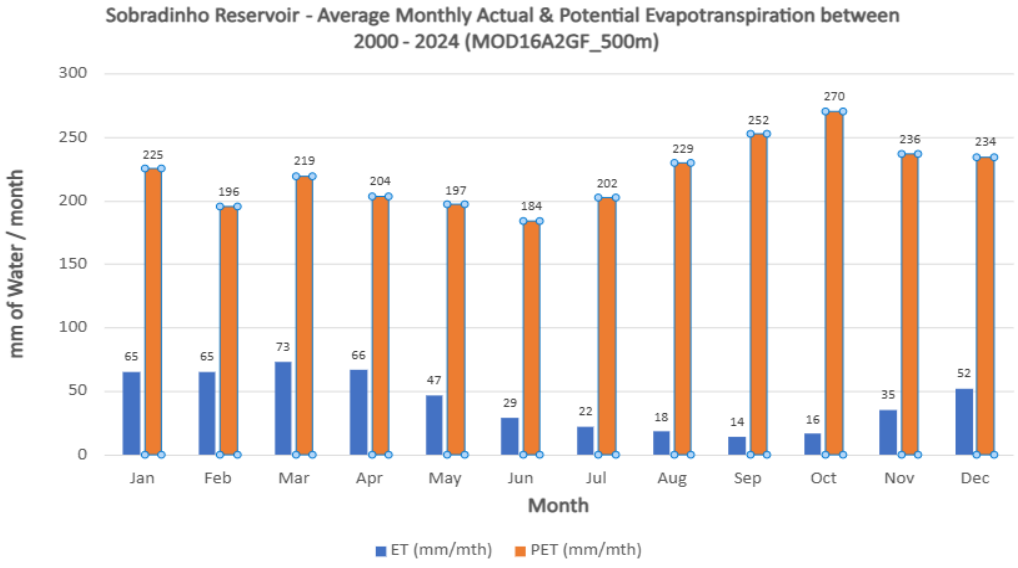

4.2.4. Seasonal Trends

Seasonal decomposition (Figure 13-13B) confirms ET dominance in JFM and suppression during JAS. PET stays high in OND and JAS when temperatures peak. During 2013-2017, both ET and PET drop significantly, revealing severe water limitation. After 2018, ET rebounds, mirroring rainfall recovery

Figures 12-13B. Seasonal ET and PET for JFM, AMJ, JAS, OND (2000-2024).

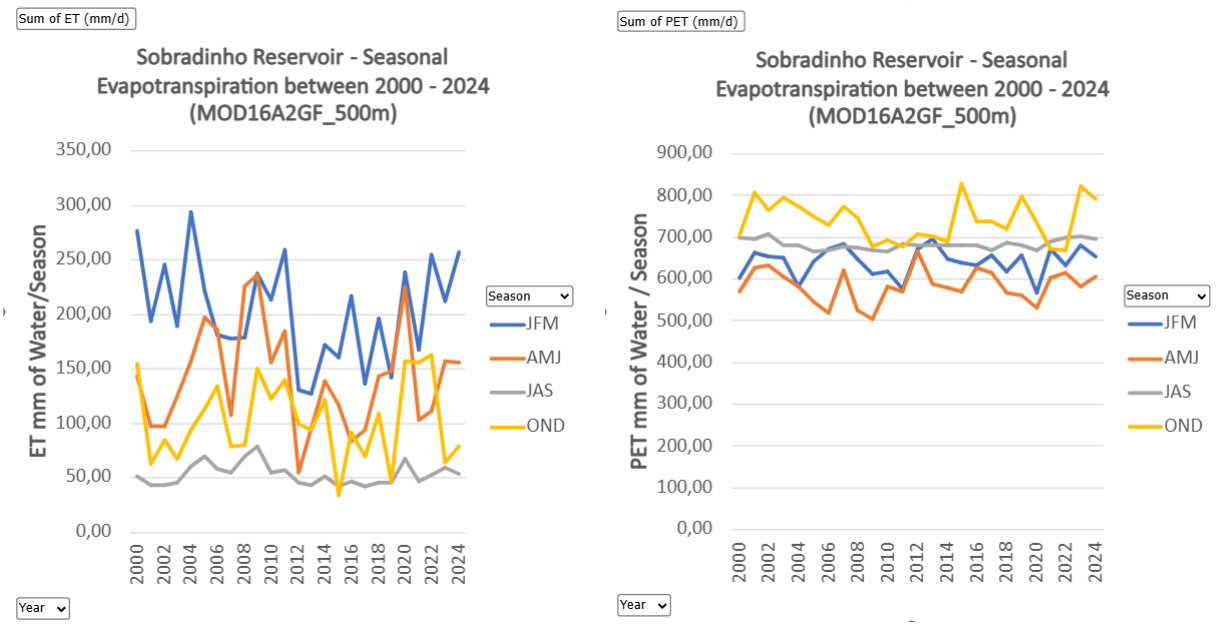

4.2.5. Evapotranspiration at Sub-Monthly Scale

The 8-day MODIS series (Figures 14-14B) captures short-term responses of ET to rainfall pulses. ET rises sharply after rain and declines quickly under dry conditions, while PET remains more stable, reflecting constant atmospheric demand.

Figures 14-14B. 8-day ET and PET variability (2000–2024).

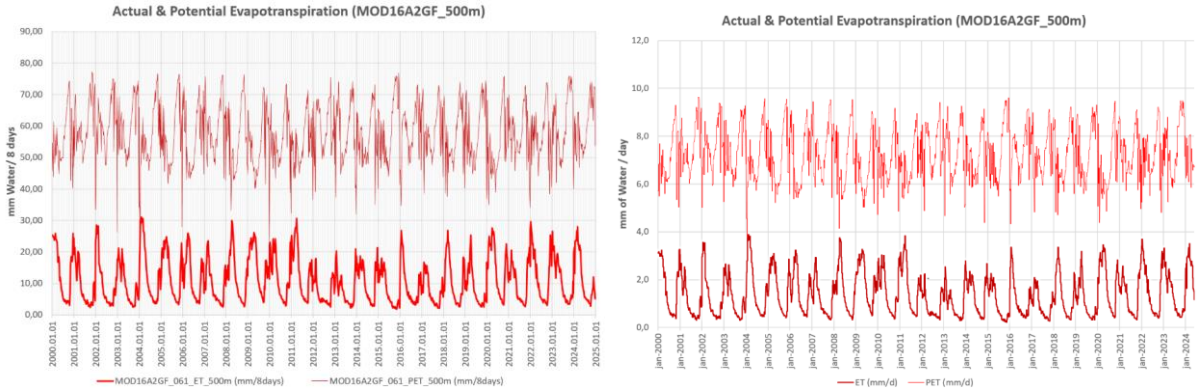

This fine-scale variability demonstrates how meteorological conditions propagate into hydrological responses at the land-atmosphere interface, with ET being a sensitive indicator of both drought onset and recovery phases.

4.2.6. Implications for Drought and Hydrological Balance

The strong coupling between ET and PET emphasizes the role of energy–moisture interactions in drought propagation across the Sobradinho system. During prolonged dryness, limited water availability suppresses ET, while high PET sustains evaporative stress and accelerates water storage decline. Post-2018, ET increases reflect improved moisture conditions and vegetation recovery, consistent with precipitation rebound. These processes contribute to the overall hydrological resilience of the reservoir, but also highlight its vulnerability to future climatic extremes, given the persistent PET-ET imbalance.

4.3. Reservoir Evaporation Losses

Evaporation from the open-water surface of the Sobradinho Reservoir is a dominant factor in its water balance. Using MODIS PET (adjusted to 80 % for open water) and CHIRPS precipitation, net annual evaporation was calculated for 2011-2024. The results were converted to volumes using an average reservoir area of 4,214 km². Potential evaporation remains stable (2,500-2,700 mm yr^{-1}), while precipitation varies (460-700 mm yr^{-1}). The net evaporation ranges from 1,300-1,740 mm yr^{-1}, corresponding to 5,400-7,300 MCM yr^{-1} of water loss. Years of lower rainfall (2012, 2015, 2019, 2023) exhibit peak evaporation, while wet years (2020) show reduced losses. These patterns reveal the sensitivity of open-water evaporation to climatic fluctuations in the semi-arid São Francisco Basin.

Figure 15. Annual PET, Precipitation, and Net Evaporation (mm yr^{-1}) for Sobradinho (2011-2024)

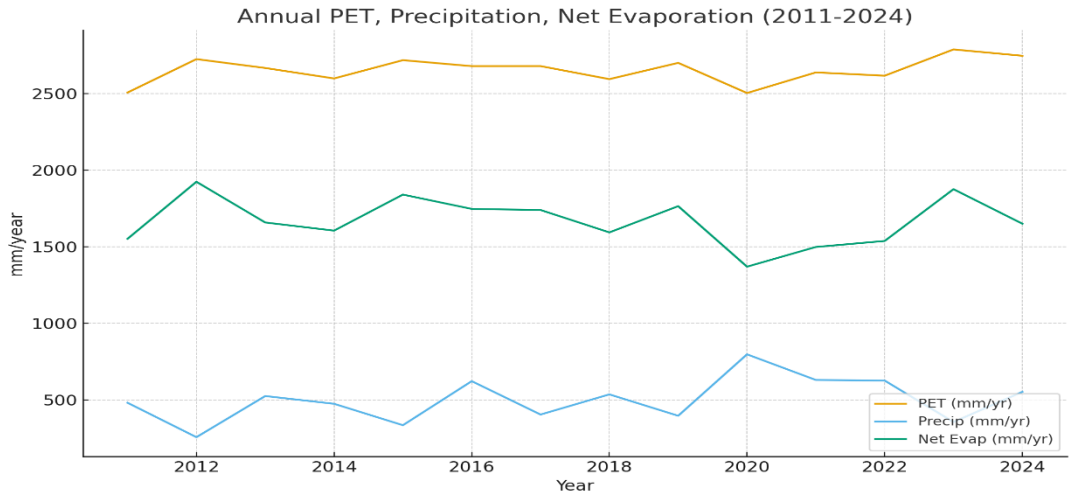

Figure 15B. Annual Net Evaporation Volume (MCM yr^{-1}) for Sobradinho (2011-2024).

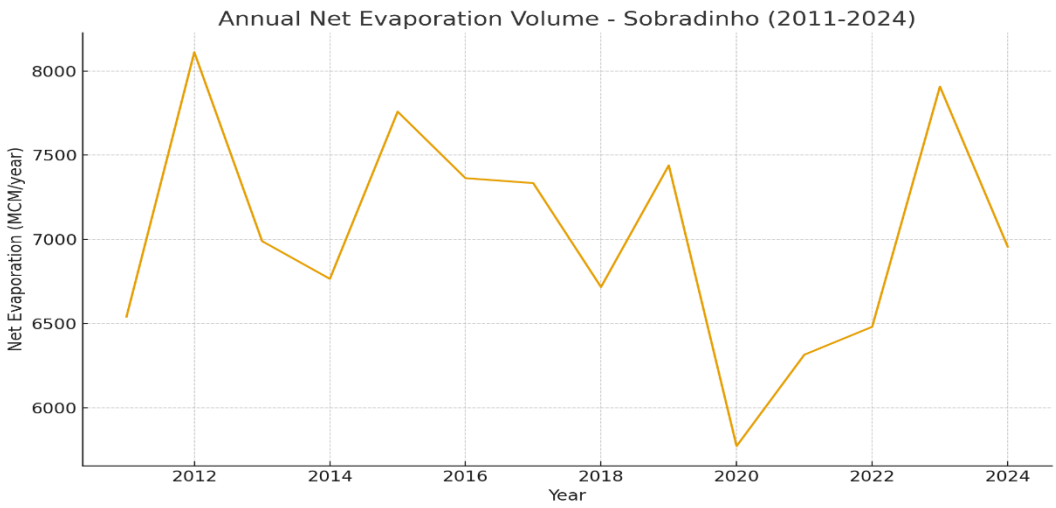

The Elevation-Area-Capacity curve of the Sobradinho Reservoir, derived from the Copernicus 30 m DEM (COP30), illustrates the relationship between water surface elevation, surface area, and storage volume (Figure 16.). The storage capacity curve (blue line) shows a steady, nearly linear increase in volume with rising elevation, reflecting the topographic shape of the reservoir basin. In contrast, the area curve (red line) indicates a sharp rise in surface area between 386 m and 388 m, likely corresponding to the water surface level captured by the DEM, where

inundated areas dominate. Above 388 m, the area stabilizes and eventually declines slightly, suggesting the presence of surrounding terrain features such as narrow valleys or rising banks. The spillway level marked at 393.5 m aligns with the upper extent of the volume curve, highlighting the reservoir's full capacity threshold and supporting the interpretation of topographic limits.

Figure 16. The Elevation-Area-Capacity curve of the Sobradinho Reservoir

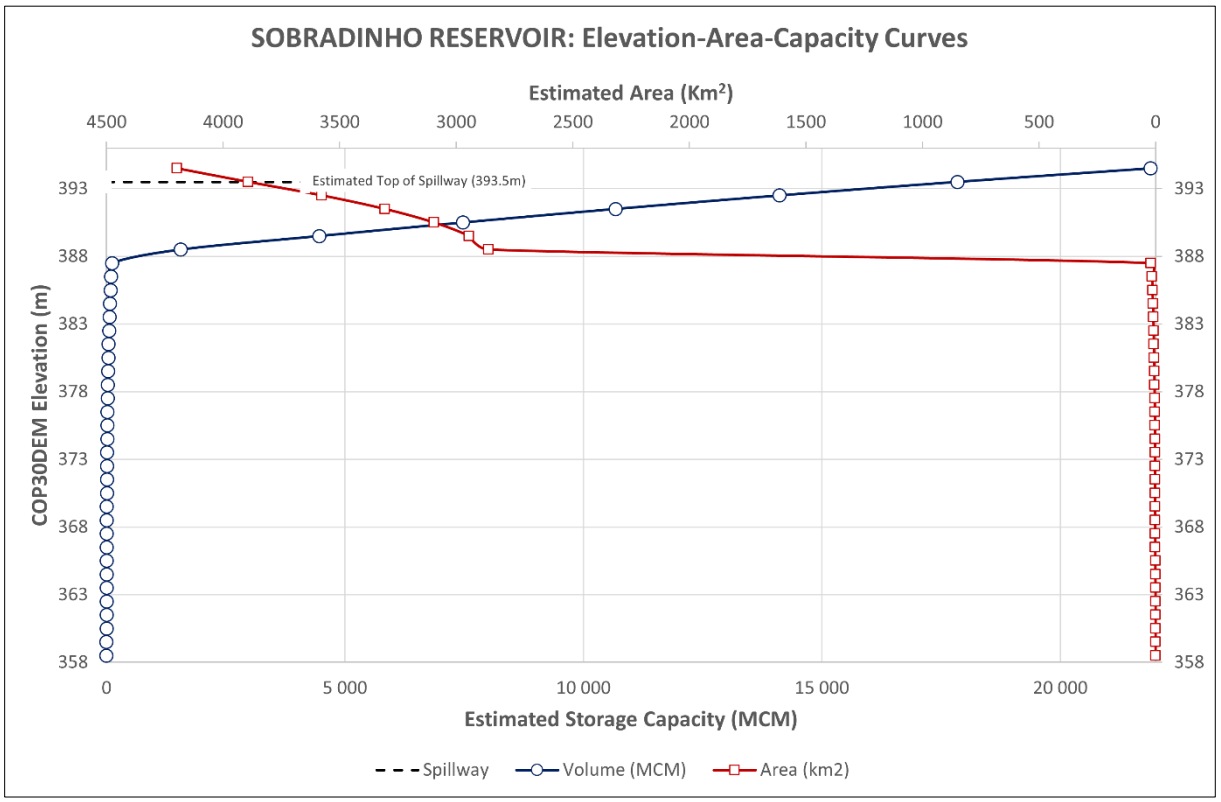

4.4. Turbidity Dynamics (2015-2017)

The turbidity patterns of the Sobradinho Reservoir, derived from the Normalized Difference Turbidity Index (NDTI), exhibit pronounced seasonal and interannual variability closely linked to rainfall, inflow, and storage fluctuations (Figure 17). During wet-season months (March 2015 and March 2017), the reservoir displays low NDTI values (darker blue tones), corresponding to clearer water conditions. Increased inflows from upstream during these periods enhance dilution and sediment deposition, resulting in reduced suspended sediment concentrations.

Figure 17. Normalized Difference Turbidity (NDTI) maps of Sobradinho Reservoir showing wet and dry seasons for 2015 and 20

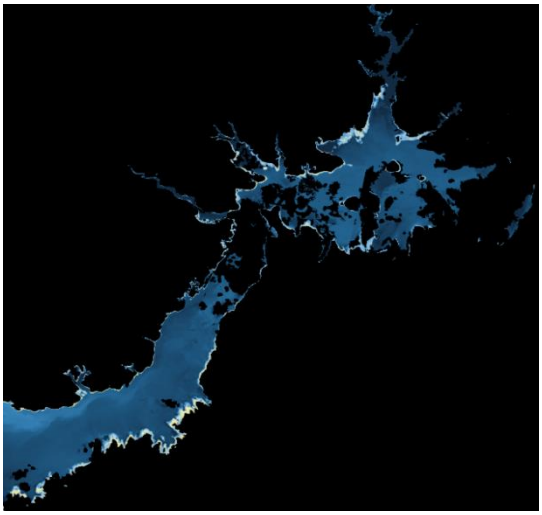

(a) March 2015 (Wet Season)

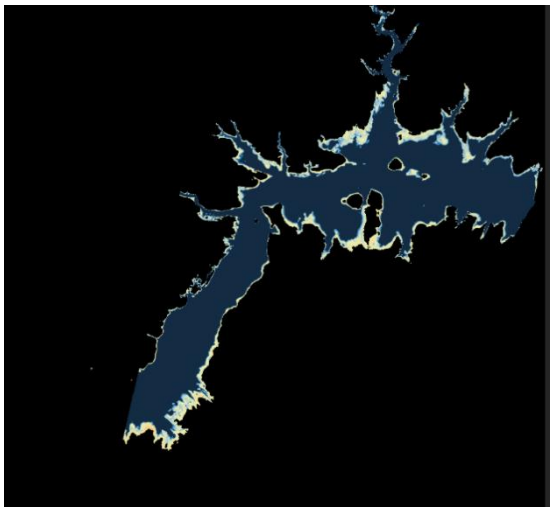

(b) September 2015 (Dry Season)

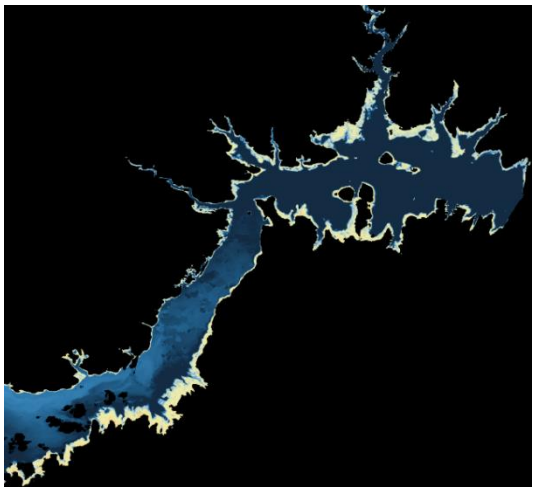

(c) March 2017 (Dry Season)

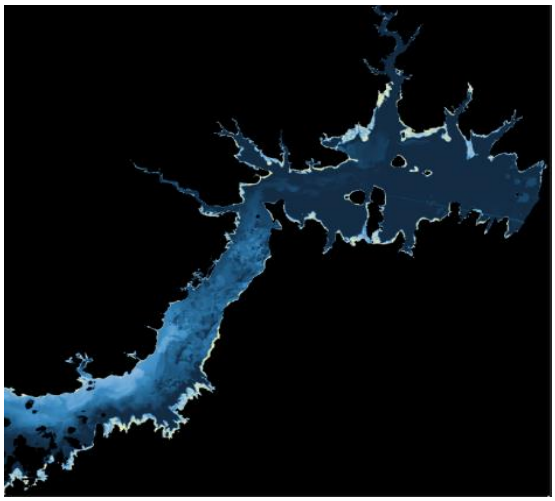

(d) September (Wet Season)

During the dry-season months (September 2015 and September 2017), the Sobradinho Reservoir exhibits visibly higher NDTI values, represented by lighter yellow to orange tones in the maps. These patterns indicate elevated turbidity and suspended sediment concentrations caused by a combination of reduced water volume, wind-induced resuspension, and shoreline erosion. As water levels decline, shallow zones become more exposed to hydrodynamic disturbance, allowing fine sediments previously deposited during wetter periods to be remobilized. The concentration of turbidity near inflow regions and reservoir margins highlights the spatial heterogeneity of sediment dynamics under drought conditions.

A comparison between 2015 and 2017 further illustrates the cumulative impact of the prolonged drought. The 2017 dry-season map reveals a greater spatial extent of high turbidity zones and

stronger NDTI responses, suggesting intensified sediment resuspension and lower water clarity. This progressive degradation aligns with the observed decrease in inflows and reservoir storage during the 2013-2017 drought period, when the Sobradinho reached historically low water levels. The differences between wet and dry seasons thus reflect both short-term hydrological fluctuations and long-term drought effects on sediment and water column stability.

Overall, these turbidity variations demonstrate that water quality in large semi-arid reservoirs is tightly coupled with climatic and hydrological conditions. Seasonal inflow pulses contribute to sediment dilution and deposition, while extended dry phases promote sediment mobilization and concentration of suspended materials.

5. Conclusions and Suggestions

The integrated analysis of satellite and climatic datasets provides new insight into the hydrological behavior of the Sobradinho Reservoir under drought variability. The combination of CHIRPS, MODIS, Landsat, and QGIS-derived elevation data proved effective for capturing multi-dimensional changes in precipitation, evaporation, water storage, and turbidity.

The results confirm that the 2013–2017 drought was the most severe event in the 21st century for the São Francisco Basin, producing extended hydrological deficits and critical reductions in reservoir inflow and volume. Despite improved rainfall after 2018, the persistence of high PET and moderate SPI/SPEI values indicates incomplete hydrological recovery. The evapotranspiration imbalance (PET $\gg$ ET) demonstrates that atmospheric demand remains the primary driver of water loss, while the elevation–capacity analysis quantifies how storage potential diminishes sharply below 388 m.

The QGIS-based morphometric analysis strengthens the understanding of reservoir sensitivity to elevation fluctuations, offering a foundation for estimating volume losses and shoreline exposure during droughts. When integrated with evaporation estimates, this approach provides a practical method for evaluating hydrological stress in large reservoirs lacking bathymetric surveys.

Turbidity analysis further reveals that water quality degradation is spatially heterogeneous and climatically driven, with sediment resuspension intensifying during low-water conditions. These findings reinforce the link between drought intensity, hydrological imbalance, and sediment dynamics.

In practical terms, the study underscores the importance of continuous remote monitoring for water management in semi-arid regions. The integration of precipitation, evapotranspiration, and elevation-based storage analysis can inform reservoir operation policies and hydropower scheduling. Future research should focus on combining satellite-derived surface elevation (e.g., altimetry or LiDAR) with hydrodynamic models to refine volume estimates and anticipate drought impacts under future climate scenarios.

6. Summary

This study investigates the hydrological and water-quality dynamics of the Sobradinho Reservoir, located in the semi-arid São Francisco River Basin of Northeast Brazil, between 2000 and 2025. The reservoir is a key component of Brazil's water and energy system but faces growing pressure from recurrent droughts and increasing water demand. The extreme drought of 2013–2017 caused one of the most critical hydrological crises in recent decades, severely reducing reservoir storage, hydropower capacity, and water availability for agriculture and local communities. Understanding these drought impacts and the reservoir's recovery is therefore essential for sustainable water management and climate adaptation in the region.

To achieve this, the research combined remote sensing, climatic indices, and geospatial analysis using Google Earth Engine (GEE), Python, and QGIS. Precipitation data from CHIRPS, evapotranspiration from MODIS (MOD16A2GF), and turbidity from Landsat 8 (NDTI) were integrated with elevation–area–capacity analysis based on the COP30 DEM. The Standardized Precipitation Index (SPI) and Standardized Precipitation–Evapotranspiration Index (SPEI) were calculated to characterize drought frequency and intensity, while reservoir water loss was estimated from PET–precipitation balances and translated into volumetric terms.

The results reveal strong interannual rainfall variability and confirm the 2013–2017 event as an extreme multi-year drought, with SPEI values below −1.5 and a collapse of normal wet-season rainfall. Evapotranspiration patterns show that PET consistently exceeded ET, reflecting sustained moisture stress typical of semi-arid systems. Annual net evaporation reached 1,300–1,740 mm yr^{-1}, equivalent to 5,400–7,300 million m^3 of water loss. The elevation–capacity curve, derived from QGIS analysis, demonstrated how reservoir storage increases sharply between 386 m and 388 m and stabilizes near the spillway elevation (393.5 m), defining the hydrological limits of the basin. Turbidity maps showed greater suspended sediment concentrations during dry periods, indicating sediment resuspension under low-water conditions and clearer water in wet seasons.

Overall, the study demonstrates that drought propagation in the Sobradinho Reservoir follows a sequential process: rainfall deficits reduce inflows, evapotranspiration declines, surface evaporation intensifies, and water quality deteriorates. The integrated use of multi-source satellite datasets proved highly effective for diagnosing these relationships. The findings highlight the reservoir's vulnerability to climatic variability and reinforce the importance of

remote-sensing–based monitoring for managing water storage, hydropower generation, and ecological sustainability in Brazil’s semi-arid regions.

7. Bibliography

Abiy, A. Z., Melesse, A. M., Seyoum, W. M., & Abtew, W. (2019). Drought and climate teleconnection and drought monitoring. In A. M. Melesse & W. Abtew (Eds.), Extreme Hydrology and Climate Variability: Monitoring, Modelling, Adaptation and Mitigation (pp. 275–295). Elsevier. https://doi.org/10.1016/B978-0-12-815998-9.00022-1

Agência Nacional de Águas (ANA). (2016). Plano de Recursos Hídricos da Bacia do Rio São Francisco 2016–2025. Brasília: ANA. https://siga.cbhsaofrancisco.org.br/sigasf/download/WebPlan/33_5b1e0b45-3360-4950-acb8-c489bf706ea6.pdf

Agência Nacional de Energia Elétrica (ANEEL). (2021). Inventário Energético Nacional – Usinas Hidrelétricas Registradas. Brasília: ANEEL.

Alkmim, F. F., & Martins-Neto, M. A. (2012). Proterozoic first-order sedimentary sequences of the São Francisco craton, eastern Brazil. Marine and Petroleum Geology, 33, 127-139. https://doi.org/10.1016/j.marpetgeo.2011.08.011

Britannica, T. E. (2024). São Francisco River. In Encyclopaedia Britannica. Retrieved from https://www.britannica.com/place/Sao-Francisco-River/Animal-life

Bacalhau, J. R., Ribeiro Neto, A., Crétaux, J.-F., & Moreira, D. M. (2022). Bathymetry of reservoirs using altimetric data associated with optical images. Advances in Space Research, 69(9), 3589–3604. https://doi.org/10.1016/j.asr.2022.01.039

Chowdhury, M., Vilas, C., van Bergeijk, S., Navarro, G., Laiz, I., & Caballero, I. (2023). Monitoring turbidity in a highly variable estuary using Sentinel-2A/B for ecosystem management applications. Frontiers in Marine Science, 10, 1186441. https://doi.org/10.3389/fmars.2023.1186441

Ciel & Terre International. (2023). Sobradinho Floating Solar Project Summary. Retrieved from https://ciel-et-terre.net/project/sobradinho

Companhia Hidro Elétrica do São Francisco (CHESF). (2022). Ficha técnica da Usina Hidrelétrica de Sobradinho. Recife: CHESF.

Comitê da Bacia Hidrográfica do Rio São Francisco (CBHSF). (2018). Relatório Técnico da Bacia do Rio São Francisco. Brasília: CBHSF.

Correia, M. F., da Silva Dias, M. A. F., & da Silva Aragão, M. R. (2006). Soil occupation and atmospheric variations over Sobradinho Lake area. Part one: An observational analysis. Meteorology and Atmospheric Physics, 94, 103–113. https://doi.org/10.1007/s00703-005-0173-4

Correia, M. F., da Silva Dias, M. A. F., & da Silva Aragão, M. R. (2006). Soil occupation and atmospheric variations over Sobradinho Lake area. Part two: A regional modeling study. Meteorology and Atmospheric Physics, 94, 115–128. https://doi.org/10.1007/s00703-005-0174-3

Climate Hazards Group. (2022). *CHIRPS: Climate Hazards Group InfraRed Precipitation with Station data (1981–present)*. University of California, Santa Barbara. Available at: https://www.chc.ucsb.edu/data/chirps

Donchyts, G. (2020). Google Earth Engine and Hydrology. Deltares. https://www.nhv.nu/wp-content/uploads/2020/08/Google-Earth-Engine-and-Hydrology_Donchyts.pdf

De Queiroz Santos, N. Q., Lima, K. C., & Spyrides, M. H. C. (2022). *The dependence of hydropower planning in relation to the influence of climate in Northeast Brazil.* PLOS ONE, 17(1), e0259951. https://doi.org/10.1371/journal.pone.0259951

Dogliotti, A. I., Ruddick, K. G., Nechad, B., Doxaran, D., & Knaeps, E. (2015). A single algorithm to retrieve turbidity from remotely-sensed data in all coastal and estuarine waters. *Remote Sensing of Environment*, 156, 157–168. https://www.sciencedirect.com/science/article/pii/S0034425714003654?via%3Dihub

D. A. Wilhite and M. H. Glantz, "Understanding: The Drought Phenomenon: The Role of Definitions," Water International, Vol. 10, No. 3, 1985, pp. 111-120. doi:10.1080/02508068508686328 https://www.scirp.org/reference/referencespapers?referenceid=919161&

Drusch, M., Del Bello, U., Carlier, S., Colin, O., Fernandez, V., Gascon, F., … & Meygret, A. (2012). Sentinel-2: ESA's optical high-resolution mission for GMES operational services. Remote Sensing of Environment, 120, 25-36. https://doi.org/10.1016/j.rse.2011.11.026

Freitas, A. A. d., Carvalho, V. S. B., & Reboita, M. S. (2021). Drought assessment in São Francisco River Basin, Brazil (1979–2020): Characterization through SPI and associated anomalous climate patterns. Atmosphere, 13(1), 41. https://doi.org/10.3390/atmos13010041

Guttman, N. B. (1999). Accepting the Standardized Precipitation Index: A calculation algorithm. Journal of the American Water Resources Association, 35(2), 311–322. https://doi.org/10.1111/j.1752-1688.1999.tb03592.x

Guedes, I. A., da Costa Neves, L., & Azevedo, S. M. F. O. (2018). Cyanobacteria and cyanotoxin occurrences in drinking water reservoirs during drought in Brazil. Water Research, 144, 603–612. https://doi.org/10.1016/j.watres.2018.08.056

Global Water Partnership (GWP) & World Meteorological Organization (WMO). (2016). Handbook of Drought Indicators and Indices (M. Svoboda & B. A. Fuchs, Eds.). Integrated Drought Management Programme (IDMP), Integrated Drought Management Tools and Guidelines Series 2, Geneva. https://www.droughtmanagement.info/literature/GWP_Handbook_of_Drought_Indicators_and_Indices_2016.pdf

International Lake Environment Committee (ILEC). (2023). World Lake Database: Sobradinho Reservoir. Retrieved from https://wldb.ilec.or.jp

Lloyd-Hughes, B., & Saunders, M. A. (2002). A drought climatology for Europe. International Journal of Climatology, 22(13), 1571–1592. https://doi.org/10.1002/joc.846

Marengo, J. A., Alves, L. M., Alvalá, R. C., Cunha, A. P., Brito, S., & Moraes, O. L. (2018). Climatic characteristics of the 2010–2016 drought in the semiarid Northeast Brazil region. *Anais da Academia Brasileira de Ciências*, 89(3), 1379–1397. https://doi.org/10.1590/0001-3765201720170206

Martins, D. M. F., Chagas, R. M., Melo Neto, J. O., & Méllo Júnior, A. V. (2011). Impacts of construction of hydroelectric plant of Sobradinho in the flow on lower São Francisco River. *Revista Brasileira de Engenharia Agrícola e Ambiental*, 15(2), 153–160. https://doi.org/10.1590/S1415-43662011001000010

McKee, T. B., Doesken, N. J., & Kleist, J. (1993). The relationship of drought frequency and duration to time scales. In Proceedings of the 8th Conference on Applied Climatology,

American Meteorological Society, 17–22 Jan 1993, Anaheim, CA (pp. 179–184). American Meteorological Society.

Martins, V2019. S., Kaleita, A., Barbosa, C. C. F., Fassoni-Andrade, A., de Lúcia Lobo, F., & Novo, E. M. L. (2019). Remote sensing of large reservoir in the drought years: Implications on surface water change and turbidity variability of Sobradinho Reservoir (Northeast Brazil). Remote Sensing Applications: Society and Environment, 13, 275-288. https://doi.org/10.1016/j.rsase.2018.11.006

McKee, T. B., Doesken, N. J., & Kleist, J. (1993). The relationship of drought frequency and duration to time scales. Proceedings of the 8th Conference on Applied Climatology, Anaheim, CA, American Meteorological Society, pp. 179–184.

McKee, T. B., Doesken, N. J., & Kleist, J. (1993). The relationship of drought frequency and duration to time scales. Proceedings of the 8th Conference on Applied Climatology, 179–184. https://www.droughtmanagement.info/literature/AMS_Relationship_Drought_Frequency_Duration_Time_Scales_1993.pdf

Nunes, L. M. F., Lürling, M., & Marques, D. M. L. M. (2022). The impact of turbidity on cyanobacterial dominance: A synthesis for tropical reservoirs. Frontiers in Environmental Science, 10, 938777. https://doi.org/10.3389/fenvs.2022.938777

National Drought Mitigation Center. (NDMC). Types of drought. University of Nebraska-Lincoln. Retrieved November 8, 2025, from https://drought.unl.edu/Education/DroughtIn-depth/TypesofDrought.aspx

Operador Nacional do Sistema Elétrico (ONS). (2023). *Hydropower generation and system operation data*. Available at: http://www.ons.org.br

Paredes-Trejo, F. J., Barbosa, H. A., Lakshmi Kumar, T. V., Thakur, M. K., & Buriti, C. O. (2021). Drought assessment in the São Francisco River Basin using satellite-based and ground-based indices. *Remote Sensing*, 13(19), 3921. https://www.mdpi.com/2072-4292/13/19/3921

Palmer, W. C. (1965). Meteorological Drought (Research Paper No. 45). U.S. Weather Bureau, Washington, D.C. https://www.droughtmanagement.info/literature/USWB_Meteorological_Drought_1965.pdf

Pekel, J. F., Cottam, A., Gorelick, N., & Belward, A. S. (2016). High-resolution mapping of global surface water and its long-term changes. *Nature*, 540(7633), 418–422. https://www.nature.com/articles/nature20584

Powers, S. M., et al. (2023). Spatially intensive patterns of water clarity in reservoirs reveal the influence of suspended particulate matter on optical water quality. Journal of Geophysical Research: Biogeosciences, 128(7), e2022JG007650. https://doi.org/10.1029/2023JG007650

Pan, Y., Guo, S., Li, Y., Li, J., & Zhu, J. (2018). Effects of water level increase on phytoplankton assemblages in a drinking water reservoir. Water, 10(3), 256. https://www.mdpi.com/2073-4441/10/3/256

Roy, D. P., et al. (2014). Landsat-8: Science and product vision for terrestrial global change research. Remote Sensing of Environment, 145, 154-172. https://doi.org/10.1016/j.rse.2014.02.028

Schmitz, M. H., Lacerda Santos, N. C., Severi, W., Gentil, E., & Gomes, L. C. (2023). Environment–ichthyofauna relations in a neotropical reservoir through a joint remote sensing/field sampling approach. Ecology of Freshwater Fish, 32(3), 571-581. https://doi.org/10.1111/eff.12707

Shuttleworth, W. J., Wallace, J. S., & McJannet, D. L. (2019). Evaporation from natural surfaces: The forgotten component of the water balance. Hydrology and Earth System Sciences.

Vicente-Serrano, S. M., Beguería, S., & López-Moreno, J. I. (2010). A multi-scalar drought index sensitive to global warming: The Standardized Precipitation Evapotranspiration Index (SPEI). Journal of Climate, 23(7), 1696–1718. https://doi.org/10.1175/2009JCLI2909.1

Vieira, N. P. A., Bueno, E. O., Pereira, S. B., & de Mello, C. R. (2018). Water footprint of the Sobradinho hydropower plant, Northeastern Brazil. Revista Ambiente & Água, 13(3), e2134. https://doi.org/10.4136/ambi-agua.2134

Van Loon, A. F. On the propagation of drought : how climate and catchment characteristics influence hydrological drought development and recovery. [internal PhD, WU, Wageningen University]. https://edepot.wur.nl/249786 (2013).

Vicente-Serrano, S. M., Beguería, S., & López-Moreno, J. I. (2010). A multiscalar drought index sensitive to global warming: The Standardized Precipitation Evapotranspiration Index. *Journal of Climate*, 23(7), 1696–1718. https://doi.org/10.1175/2009JCLI2909.1

Van Den Hoek, J., Getirana, A., Jung, H. C., Okeowo, M. A., & Lee, H. (2019). Monitoring reservoir drought dynamics with Landsat and radar/lidar altimetry time series in persistently cloudy eastern Brazil. Remote Sensing, 11(7), 827. https://doi.org/10.3390/rs11070827

Xu, H. (2006). Modification of normalized difference water index (NDWI) to enhance open water features in remotely sensed imagery. *International Journal of Remote Sensing*, 27(14), 3025–3033. https://www.tandfonline.com/doi/full/10.1080/01431160600589179

Wang, H., Zhao, Y., & Fu, W. (2023). Utilizing the Sobol' sensitivity analysis method to address the multi-objective operation model of reservoirs. *Water*, 15(2), 389. https://doi.org/10.3390/w15020389

8. List of figures and tables

9. Acknowledgements

First and foremost, I thank God for granting me strength, perseverance, and guidance throughout this journey. Without faith and determination, the completion of this work would not have been possible.

I extend my deepest gratitude to my supervisor, György Kerezsi, for his valuable guidance, patience, and continuous support instrumental in shaping this thesis. His expertise and encouragement have greatly contributed to both my academic and personal growth.

I also wish to express my sincere appreciation to the University of Agriculture and Life Sciences, MATE (Gödöllő, Hungary), and to the Institute of Environmental Sciences for providing an exceptional academic environment and access to the resources necessary to complete this research.

My heartfelt thanks go to all the professors and lecturers who have shared their knowledge and inspired me throughout my studies, and to my classmates and colleagues for their friendship, motivation, and cooperation during this academic journey.

Finally, I dedicate this achievement to my family and loved ones for their unconditional love, encouragement, and unwavering belief in my potential. Their support has been my greatest source of strength.

10. Declarations

MATE Organizational and Operational Regulations
III. Requirements for Students
III.1. Study and Examination Regulations
Appendix 6.13: The MATE Uniform Thesis /thesis / final thesis / portfolio guidelines
Annex 4.2: Declaration of public access and authenticity of the thesis/thesis/dissertation/portfolio

DECLARATION

the public access and authenticity of the thesis

Student's name:	Menezes Sá Tarcísio Henrique
Student's Neptun code:	GEB20U
Title of thesis:	GEOSPATIAL AND HYDROLOGICAL ASSESSMENT OF SOBRADINHO RESERVOIR
Year of publication:	2025
Name of the consultant's institute:	Institute of Environmental Sciences
Name of consultant's deparment:	Department of Environmental Analytics and Environmental Technology

I declare that the final thesis/thesis/dissertation/portfolio[1] submitted by me is an individual, original work of my own intellectual creation. I have clearly indicated the parts of my thesis or dissertation which I have taken from other authors' work and have included them in the bibliography. Furthermore, I declare that the artificial intelligence tools (e.g. text generation, linguistic correction, translation, data analysis) used during the preparation of the thesis did not substitute my own research and creative work; their use was indicated either in the list of sources or in the methodology section, and I acted in accordance with professional and ethical expectations.

If the above statement is untrue, I understand that I will be disqualified from the final examination by the final examination board and that I will have to take the final examination after writing a new thesis.

I do not allow editing of the submitted thesis, but I allow the viewing and printing, which is a PDF document.

I acknowledge that the use and exploitation of my thesis as an intellectual work is governed by the intellectual property management regulations of the Hungarian University of Agricultural and Life Sciences.

[1] While keeping the appropriate thesis type, all other types are to be removed.0

I acknowledge that the electronic version of my thesis will be uploaded to the library repository of the Hungarian University of Agricultural and Life Sciences. I acknowledge that the defended and

- not confidential thesis after the defence
- confidential thesis 5 years after the submission

will be available publicly and can be searched in the repository system of the University.

Date: 2025.11.11

Student's signature

Declaration of Students and Doctoral Candidates on the Use of Artificial Intelligence (AI)"

1. general information:

Name of the student:	**Menezes Sá Tarcísio Henrique**
Neptun ID:	**GEB20U**
Level of program (mark with X):	X BSc/BA ☐ MSc/MA ☐ Doctoral School (PhD) ☐ Other: ……
Name and code of the subject*:	**Thesis Work – KORTU132N**
Title of the work:	**GEOSPATIAL AND HYDROLOGICAL ASSESSMENT OF SOBRADINHO RESERVOIR**

* Not required to be completed in the case of a doctoral dissertation.

2. Declaration on the Use of AI

I, the undersigned, fully aware of my ethical responsibility, make the following declaration:

(Please choose one of the options below!)

☐ A) I have not used any artificial intelligence system or service.

(If you selected this option, completing the subsequent tables is not required.)

X B) I have used an artificial intelligence system or service.

(Please fill in the relevant tables!)

3. Details of Artificial Intelligence Usage

TABLE I: Assistant or Minor Usage (e.g., translation, language proofreading, brainstorming, etc.)

(For these uses, attaching the specific prompts and responses is not required.)

Purpose of Use	**Name and Version of the AI Tool Used**	**Affected Section (if not applicable to the entire text)**
Proofreading, brainstorming, grammar correction, explanations, coding, code debugging, and paraphrasing sentences	ChatGPT 5, Scopus AI, and Quillbot	

TABLE II: Significant Content Contribution (e.g., generating an entire figure or a longer text section)

(In these cases, documenting the key prompts used and the raw responses provided by the AI, and attaching them as an appendix to the work, is required.)

Purpose of Use	**Name, Version, and Access Information of the AI Tool Used**	**Exact Number of the Affected Chapter / Figure / Table**	**Entry Number of the Appendix Containing the Prompt Log**

3/A. Additional Rules Prescribed by the Lecturer (if any)

If the instructor or supervisor of the course has established specific rules or expectations regarding the use of AI tools, please summarize them in the field below:

For example: prohibition of AI use for certain types of tasks; only specific tools are permitted; different citation requirements; documentation format, etc.

Rules Prescribed by the Lecturer or Supervisor

……

……

……

……

4. Declaration Applicable to All Students:

I declare that I have critically reviewed, edited, and incorporated any content potentially generated by AI in all cases. I take full responsibility for every element of the submitted work, including its originality and scientific validity. I acknowledge that the Hungarian University of Agriculture and Life Sciences may check the submitted work with an artificial intelligence detector and may initiate proceedings if my declaration is found to be false or incomplete.

Place and Date: Gödöllő, 2025. 11. 11.

....

Signature of the Student **Signature of the Advisor/Supervisor**

DECLARATION

György Kerezsi (student Neptun code: GEB20U) as a consultant, I declare that I have reviewed the thesis and that I have informed the student of the requirements, legal and ethical rules for the correct handling of literary sources.

I <u>recommend</u> / do not recommend[2] the thesis to be defended in the final examination.

The thesis contains a state or official secret: yes <u>no</u>*[3]

Date: 2025.11.11

Kerezsi György

[2] The appropriate one should be underlined.
[3] The appropriate one should be underlined.